BIOCYBERNETICS AND BIOMEDICAL ENGINEERING 41 (2021) 352–361

Available at www.sciencedirect.com

ScienceDirect

journal homepage: www.elsevier.com/locate/bbe

Original Research Article

Metameric representations on optimization of nano particle cancer treatment

Michail-Antisthenis Tsompanas [a,*], *Larry Bull* [b], *Andrew Adamatzky* [a], *Igor Balaz* [c]

[a] *Unconventional Computing Laboratory, University of the West of England, Bristol, UK*
[b] *Department of Computer Science and Creative Technologies, University of the West of England, Bristol, UK*
[c] *Laboratory for Meteorology, Physics and Biophysics, Faculty of Agriculture, Trg Dositeja Obradovica 8, University of Novi Sad, Novi Sad, Serbia*

ARTICLE INFO

Article history:
Received 11 July 2020
Received in revised form
8 February 2021
Accepted 16 February 2021
Available online 6 March 2021

Keywords:
Metameric genetic algorithms
Variable-length genetic algorithms
Cancer treatment
Nano-particles
PhysiCell

ABSTRACT

In silico evolutionary optimization of cancer treatment based on multiple nano-particle (NP) assisted drug delivery systems was investigated in this study. The use of multiple types of NPs is expected to increase the robustness of the treatment, due to imposing higher complexity on the solution tackling a problem of high complexity, namely the physiology of a tumor. Thus, the utilization of metameric representations in the evolutionary optimization method was examined, along with suitable crossover and mutation operators. An open-source physics-based simulator was utilized, namely PhysiCell, after appropriate modifications, to test the fitness of possible treatments with multiple types of NPs. The possible treatments could be comprised of up to ten types of NPs, simultaneously injected in an area close to the cancerous tumour. Initial results seem to suffer from bloat, namely the best solutions discovered are converging towards the maximum amount of different types of NPs, however, without providing a significant return in fitness when compared with solutions of fewer types of NPs. As the large diversity of NPs will most probably prove to be quite toxic in lab experiments, we opted for methods to reduce the bloat, thus, resolve to therapies with fewer types of NPs. Namely, the bloat control methods studied here were removing types of NPs from the optimization genome as part of the mutation operator and applying parsimony pressure in the replacement operator. By utilizing these techniques, the treatments discovered are composed of fewer types of NPs, while their fitness is not significantly smaller.

1. Introduction

Cancer treatment based on chemotherapy have made great progress during the past decades. Despite that, there is still room for improvement, given that cancer remains as one of the most challenging and complicated problems that scientists have faced. As nanotechnology is more broadly studied and fabrication processes more approachable, the use of

* Corresponding author at: University of the West of England.
E-mail address: Antisthenis.Tsompanas@uwe.ac.uk (M.-A. Tsompanas).
https://doi.org/10.1016/j.bbe.2021.02.002

nanocarriers has been brought into the fight against cancer [1,2]. A characteristic example is the functionalization of nano-particles (NPs) with a therapeutic compound that have proved to enhance the biodistribution, tumour penetration and cellular uptake in targeted tissues [3–6]. The fact that functionalized NPs improve the efficacy of the conventional treatment have been proved in several cases by studies *in vivo*, *in vitro* and both [7–9].

The physiology of a cancer tumor can be characterised as complicated and constantly changing [10,11]. The existence of multiple types of cancerous cells in a tumor, like Cancer Stem Cells (CSCs) [12,13], can be associated with its ability to relapse and essentially withstand conventional treatments. Moreover, when CSCs are further stressed with the application of a treatment, they seem to become more aggressive, mutate and render the applied treatment obsolete [14–16]. As a consequence, to produce more robust future cancer therapies, they will have to be more complex or adaptable to the evolution of their target. For instance, NP based therapies have been proposed able to combine photothermal and immune strategies [17], able to transfer tumor antigens and adjuvants to the same immune cells in order to effectively promote immune responses [18] or able to combine the functionality of radiation dose enhancer and anticancer drug delivery [19].

A further step towards this direction would be to incorporate more than one types of NPs in NP-based drug delivery systems [20–22]. Thus, different types of NPs will give rise to diverse behaviours of the therapy, targeting multiple aspects of the tumor and even enable the emerging of more complicated behaviours than a simple accumulation of isolated ones [23,24]. Note that rather than combining multiple drugs in one NP [25], each drug will have a different type of NP as a carrier to achieve different accumulation, retention, and penetration characteristics.

In order to study the effects of multiple types of NPs in drug delivery, the simulation of the growth of a cancerous tumour and its reaction to a multiple NP therapy was investigated *in silico*. There are several attempts to simulate the effects of nanomedicine on tumors and their microenvironment [26–28] or the mechanism that determine the cell-particle interaction and uptake [29], but here PhysiCell [30] was utilized. PhysiCell is an open-source, physics-based cell simulator. Appropriate alternations in the source code were made to accommodate the inclusion of multiple types on NPs in the therapy. The optimization problem is then formulated, with an objective function defined as the minimization of the remaining cancer cells in the tumor after 3 days of simulated treatment and a search space outlined by the parameters of the simulator that dictate the behaviour of the different types of NPs.

The fact that more than one types of NPs can be tested, without knowing *a priori* the optimum amount of different types, requires a variable length representation of the genome of each solution. As a result, the metameric representation [31,32] was adopted with the relevant variations on the operators of the evolutionary methodology.

Several optimization methodologies were previously investigated by utilizing PhysiCell to obtain a fitness function, either by testing NP-based therapies [33–36] or exploring the space of immunotherapies [37]. However, here the search space is more complicated than in the previous works on optimization of NP-based therapies, as more than one NPs are investigated. A previous study [38] has tested the problem of multiple NPs, nevertheless, the optimization evolution was implemented only by a modified mutation operator, which can be a slow way of exploring the search space. In this study, not only the mutation, but also the crossover operator were adapted to comply with a variable length genome in the evolutionary process. Moreover, another work [39] presents the investigation of multiple NPs in a single treatment, however, in that study the time that the different types of NPs are applied is not the same. Thus, the additional time variation of NPs increases the complexity of the cancer treatment.

The results clearly suffered from bloat, namely the amount of types of NPs of the evolved solutions was increasing and reaching the maximum, without a significant benefit in terms of fitness [40]. Consequently, appropriate alternations in the optimization methodology were implemented to control the bloat phenomena. Namely, the mutation operator was not only adding, but also removing types of NPs, with the same probability between the two moves. Additionally, the replacement operator was amended to apply parsimony pressure [41], specifically, to favor treatment solutions with fewer types of NPs. By utilizing these changes the treatments found were clearly less complex than the previous ones.

2. Metameric representation in genetic algorithms

Given that the amount of types on NPs that will provide the most efficient treatment is not known *a priori*, a variable length genome optimization method is required. Due to the specifics of this problem, each solution can be described as a group of parameters that are repeated, resulting in a genome composed of similar compartments. Namely, two different solutions/treatments are illustrated in Fig. 1, where one solution is comprised by 4 types of NPs and the other by 6 types of NPs. Note that each type of NPs is defined by five parameters, each one has different values for the different types of NPs. Every genome compartment is defining one type

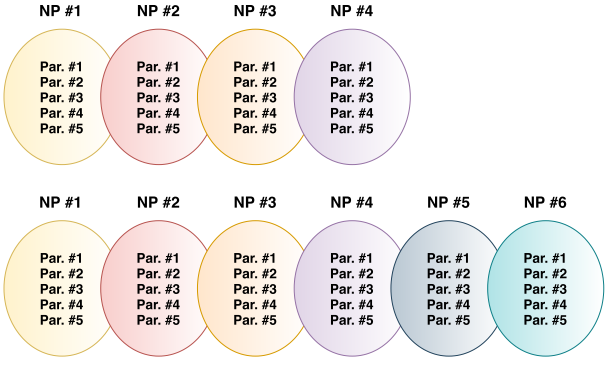

Fig. 1 – Metameric representation of two different treatments, one with 4 types of NPs and one with 6 types of NPs. All types of NPs are defined by a group of 5 parameters (different values for every type of NP).

of NPs in the simulated treatment. This representation is known as metameric representation [31,32] and each compartment as a metavariable. Similar techniques have been applied to problems from other fields, like designing wind farms [42] or positioning nodes in a coverage network [43].

Note that by altering the representation of the possible solutions, the conventional fixed-length operators can not be applied without appropriate alternations. Specifically, the updated crossover and mutation operators could change the number of types on NPs in a solution (or the length of the genome). As the crossover operators in evolutionary algorithms need to maintain the building blocks of the fit individuals of previous generations, and the fact that these blocks can be considered here as a combination of some types of NPs, the operator is designed accordingly. The "cut and splice crossover" operator was adopted, as it is a simple variation of the conventional *n*-point crossover, but the cut points are allowed only between separate metavariables. In essence, the individuals under the crossover operator exchange some types of NPs between them, but not necessarily the same amount each. An example of this crossover operator is depicted in Fig. 2.

Moreover, the mutation operator in the metameric representations is slightly altered. It is capable of altering one parameter of one type of NPs (mutation type 1 in Fig. 3) or add an additional type of NPs (with random parameters) in the mutated individual/solution (mutation type 2 in Fig. 3). Both alternatives have the same probability of happening. Thus, the mutation operator is the only way to modify the individual parameters of any type of NPs from their initial values, given that the crossover operator applies cut points only between metavariables.

As these operators, usually tend to increase the genome length uncontrollably, but without significant advances in the relative fitness (bloat), techniques to control this can be utilized. Here, in addition to adding a type of NPs, the mutation operator can also remove it. Moreover, parsimony pressure was applied to the replacement operator. More specifically, during the replacement procedure of the algorithm, if the offspring that is tested to replace a parent is of higher genome length, it also needs to be fitter at least 10%,

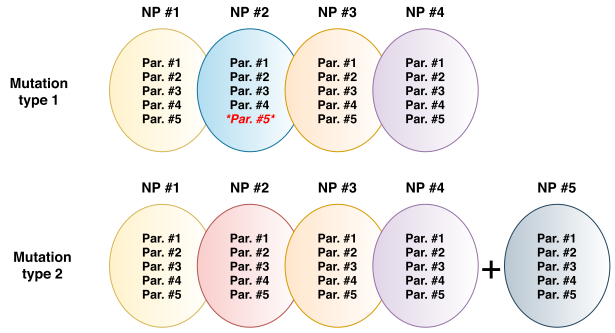

Fig. 3 – Two types of alternations by mutation operator. Type one changes one parameter on one types of NP, while type two adds a random type of NPs to the treatment.

otherwise the replacement does not happen. On the contrary, if the offspring has the same or shorter length than a parent, then their fitnesses are compared without any weighted effect.

In order to shrink the primary search space and enable the gradual advancement of complexity in solutions, the initialization of the population was opted for individuals with only one type of NPs. A similar strategy was successfully adopted previously [44] to control bloat in early generations and enhance the convergence to optima.

3. Methods

To simulate the behaviour of complex NP-based cancer treatments, PhysiCell [30], a multicellular, agent-based simulator was utilized. Namely, the sample project of PhysiCell v.1.7.0 [45], termed 2-D "anti-cancer biorobots" was used. This project simulates nanocarriers as mediators of the same chemotherapeutic compound through three different types of agents, specifically cancer cell, worker and cargo agents. Note that the cancer cell agents are encoded with the behaviour of cancer cells, while the cargo agents are corresponding to the therapeutic compound in the simulator. The worker agents are the simulated entities that associate to

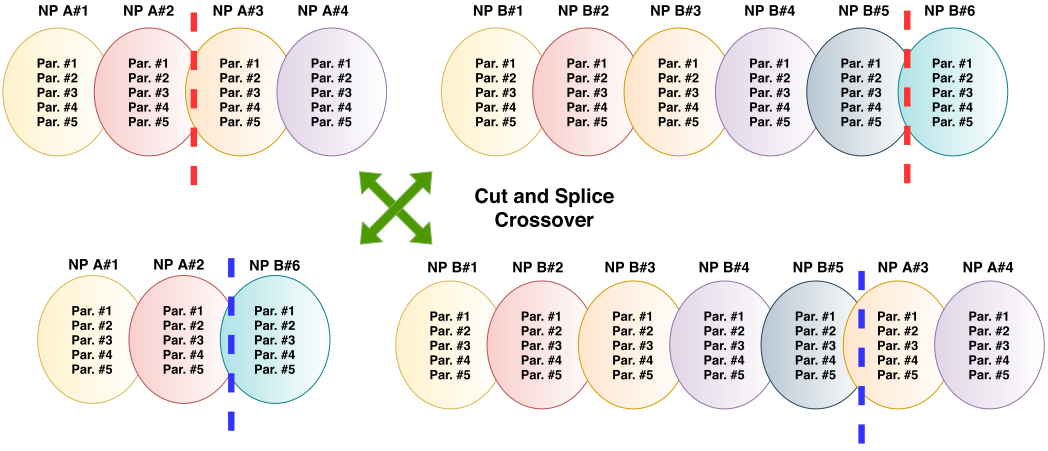

Fig. 2 – The cut and splice crossover of two treatments. On the top the parent individuals are presented with the cut points indicated in red dashed lines, while the offspring is on the bottom.

the NPs. In detail, cancer agents consume oxygen that stems an oxygen gradient. This is "read" by worker agents to inform them for targeting. Moreover, worker agents adhere to cargo agents and transport them close to cancer agents. The simulated behaviour of the worker agents is altered during the optimization process by the following five parameters, that compose the search space for each type of NPs: the unattached worker migration bias [0,1]; the attached worker migration bias [0,1]; worker relative repulsion [0,10]; worker relative adhesion [0,10]; worker motility persistence time (minutes) [0,10]. For details of the meaning of these parameters refer to [30].

The simulated procedure of this project is as follows. Note that all the following parameters are maintained the same as the original version [45]. An initial 200 μm radius tumor (or around 570 of cancer cell agents) is the starting point of the simulation, in the center of a simulation area of $1400 \times 1400 \mu m$. The growth of this tumor is simulated for seven days. At that point, the therapy is introduced close to the tumor, filling a simulated vein at coordinates $[600 \cdots 700, -700 \cdots 700]$. The therapy is comprised by 500 agents, 90% being therapeutic compound (simulated cargo agents) and 10% being NPs (simulated worker agents). After that, three days of simulated time are executed for the therapy to work. That is achieved by the functionality that worker agents have, i.e. to adhere to cargo agents and deposit them near cancer cell agents, which decay and die due to the proximity to the cargo agents. The fitness of the simulated treatment is considered as the alive remaining cancer cell agents after the end of the total of 10 days. Thus, the optimization problem can be formulated as the minimization of the fitness function, namely:

$$\min_{x} f(x) = \sum_{t=10\text{days}} (\texttt{Alive\_cancer\_agents}) \tag{1}$$

where x is the set of parameters defining the NP design, within bounds:

$$\begin{cases} 0 \leqslant & migration\_bias_{\texttt{attached\_worker}} \leqslant 1 \\ 0 \leqslant & migration\_bias_{\texttt{unattached\_worker}} \leqslant 1 \\ 0 \leqslant & relative\_adhesion_{\texttt{worker}} \leqslant 10 \\ 0 \leqslant & relative\_repulsion_{\texttt{worker}} \leqslant 10 \\ 0 \leqslant & motility\_persistence\_time_{\texttt{worker}} \leqslant 10(min) \end{cases}$$

As this is an open-source tool, appropriate alternations were introduced to accelerate the computations and enable the injection of multiple types on NPs rather than one. Initially, instead of simulating the cancer tumor growth for seven days and then introducing the therapy, an already grown tumor is loaded as the initial state and at $t = 0$ the therapy is introduced [36]. This results in a 70% acceleration of each simulation. A maximum of ten different types of NPs can be now introduced simultaneously as part of the therapy. Note here that the amount of worker agents (the simulated NPs) is not altered. Still a total of 50 worker agents were introduced, equally divided among the different types of NPs tested. For instance, if one type of NPs is tested, all 50 worker agents have the same parameters, if two types of NPs are tested, 25 worker agents have the same parameters and the rest 25 worker agents have different parameters, and so on. The pseudocode of the treatment injection procedure is given in Algorithm 1.

Algorithm 1.: Injection of multiple NP treatment.

```
Data: T_num: Amount of treatment injected agents (worker and cargo agents)
Data: W_fr(0 − 9): Fraction of 10 types of differentiated worker agents
for i ← 1 to T_num do
    if i < T_num * W_fr(0) then
        Insert one worker agent with ID0;
    else if T_num * W_fr(0) ≤ i < T_num * (W_fr(0) + W_fr(1)) then
        Insert one worker agent with ID1;
    else if
     T_num * (W_fr(0) + W_fr(1)) ≤ i < T_num * (W_fr(0) + W_fr(1) + W_fr(2))
     then
        Insert one worker agent with ID2;
    else if ... then
        ...
    else
        Insert one cargo agent ;
    end
    T_num − = 1;
end
```

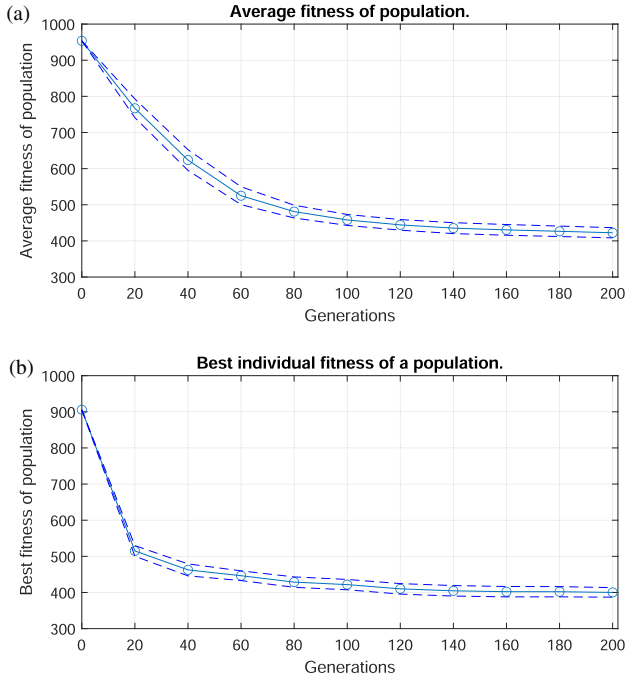

Fig. 4 – Average and confidence levels (95%) results from 10 runs of GA with metameric representation: (a) Evolution of average fitness of the population; (b) evolution of the best individual in the population.

Simulating ten days requires c. 5 min. on an Intel® Xeon® CPU E5-2650 at 2.20 GHz with 64 GB RAM using 8 of the 48 cores, while with the alternation of loading the tumor, it requires c. 1.5 min. Additionally, as the simulator is based on stochastic processes, a static sampling approach was employed by averaging the fitness of five runs for every solution tested in the optimization process. Note that all the parameters are fixed (i.e. amount of NPs, distance of injection, initial tumour size) except the five mentioned previously that can depict a different design of NPs.

A steady state genetic algorithm was implemented to optimize the design of the treatment. A randomly initiated population of size $P = 20$ was produced with each individual/solution having only one type of NPs, as explained before, to minimize the initial search space and solution complexity. The selection and replacement were executed with tournaments of size $T = 2$. The mutation operator is applying, with probability $p = 50\%$, an alternation in one of the parameters (with random step size of $s = [-5; 5]\%$) or an addition of a random type of NP in the individual. Finally, 200 generations are executed, meaning a total of 1000 PhysiCell simulations (due to the static sampling of 5), resulting to c. 25 h of execution time per evolutionary test.

4. Results

4.1. *Results of the metameric representation*

The results of ten runs of the evolutionary optimization of the multiple-NP-based drug delivery system for cancer treatment with the genetic algorithm with metameric representation

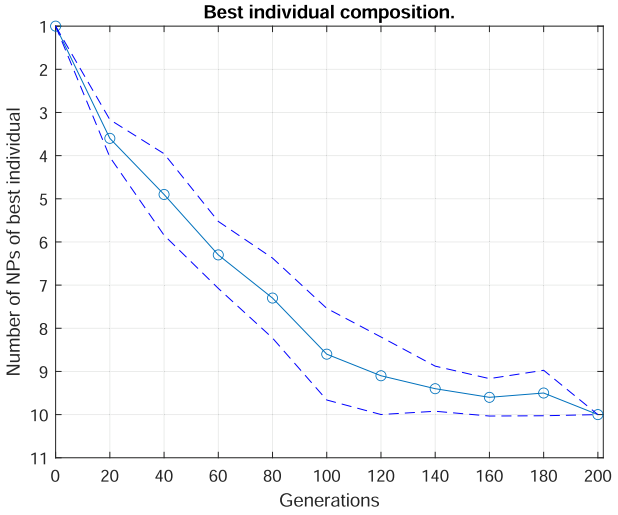

Fig. 5 – Average and confidence levels (95%) results from 10 runs of GA with metameric representation for the NP types composition of the best solution.

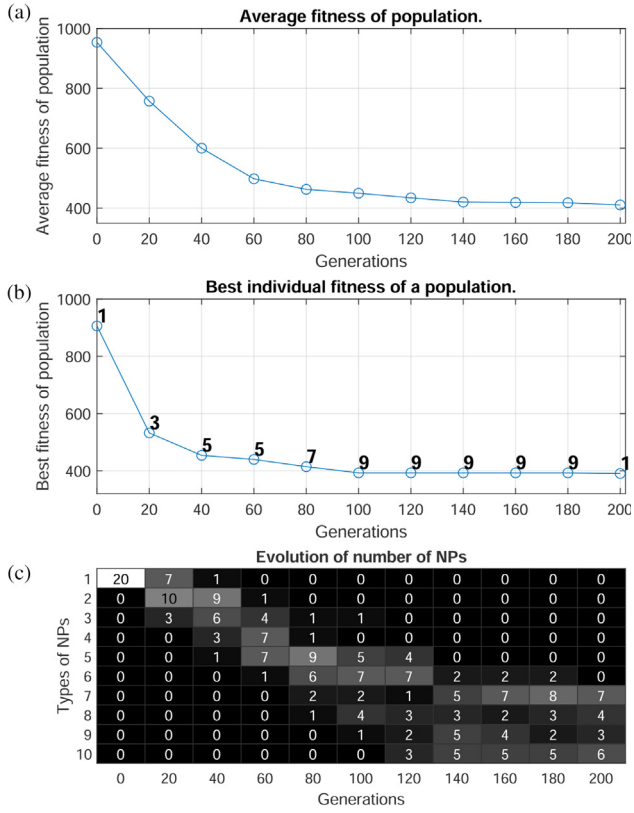

Fig. 6 – Results from one run of GA-MR. (a) Evolution of average fitFig. 6 – Results from one run of GA-MR. (a) Evolution of average fitness of the population; (b) evolution of the best individual in the population (where numbers indicate the number of types NPs); (c) composition of

(GA-MR) are depicted in Fig. 4. In Fig. 4(a) the average fitness of the population and the confidence levels (95%) of the results for 10 runs are outlined. In Fig. 4(b) the fitness of the best individuals are presented during the 200 generations of

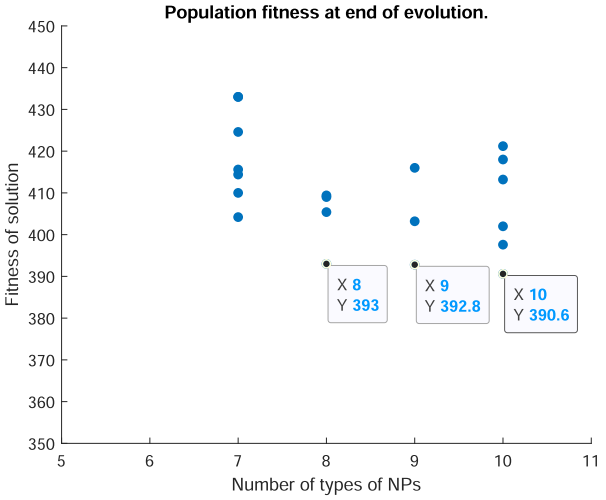

Fig. 7 – Fitness of individuals in the end of the evolutionary process in accordance with the number of types of NPs in each population.

the evolution. Furthermore, the composition of the best solution of the population, in terms of the amount of different NP types, throughout the evolution generations is illustrated in Fig. 5. The average amount of types for the 10 runs is depicted, as well as the 95% confidence levels.

In Fig. 6(a) and (b) the average fitness of the population and the fitness of the best individual are depicted for one example run of *GA-MR*. Additionally, in Fig. 6(b) the composition of each best solution per generation is depicted as a number by the data point in the graph. In Fig. 6(c) the composition of the population in terms of types of NPs is rendered. Namely, the matrix shows the number of different types of NPs of each individual/solution per depicted generation. For instance the initial population has 20 individuals that each one has one type of NP, whereas in the last generation the population has 7 individuals with 7 types of NPs, 4 individuals with 8 types of NPs and so forth. Fig. 7 shows the resulting fitness of the population of 20 individuals at the end of the evolution, after 200 generations. In *x*-axis the composition of the individual solution is sketched, while in *y*-axis the fitness of the corresponding solution.

4.2. *Results with parsimony pressure*

Here the results from an updated methodology are presented. Namely, parsimony pressure was included in the replacement operator (genetic algorithm with metameric representation and parsimony pressure *GA-MRPP*). As explained in Section 2, a weight of 10% more effective behaviour needs to be presented by a new individuals with longer genome lengths, in order to replace old individuals existing in the population. Moreover, the mutation operator was updated to remove, as well as add one random type of NPs, that serves as an additional measure against bloat.

The results of ten runs of the optimization methodology with parsimony pressure, are depicted in Fig. 8. Fig. 8(a) presents the optimization of the average fitness of the population and Fig. 8(b) illustrates the fitness of the best individuals dur-

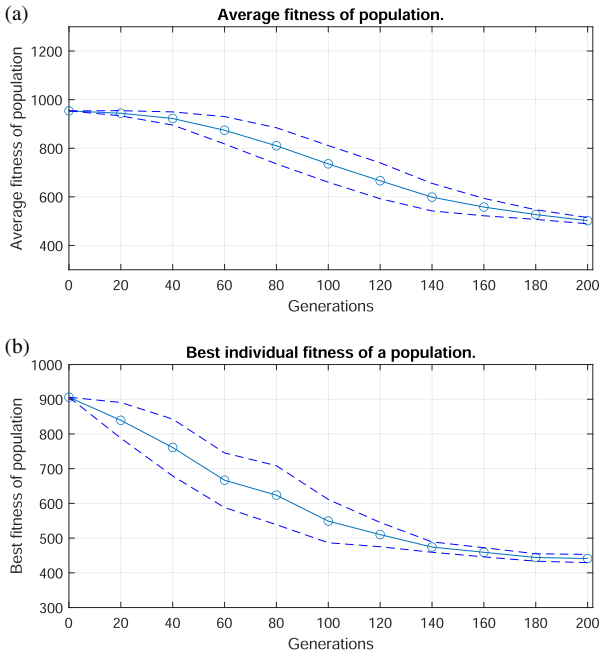

Fig. 8 – Average and confidence levels (95%) results from 10 runs of GA with metameric representation and parsimony pressure; (a) Evolution of average fitness of the population; (b) evolution of the best individual in the population.

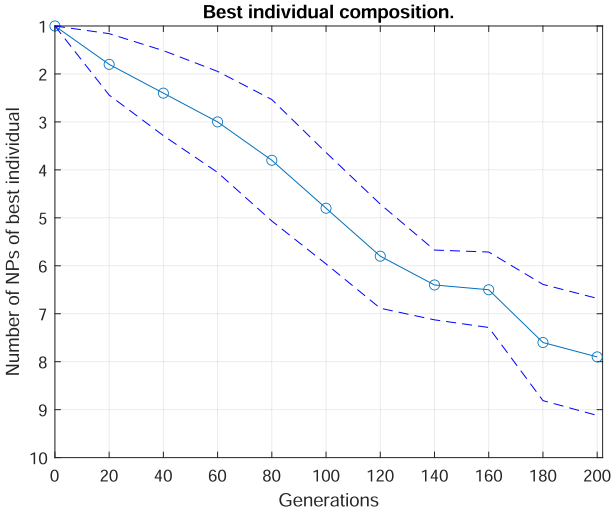

Fig. 9 – Average and confidence levels (95%) results from 10 runs of GA with metameric representation and parsimony pressure for the NP types composition of the best solution.

ing the 200 generations. Moreover, the composition of the best solutions in a population, in terms of the amount of different NP type, is illustrated in Fig. 9. The average amount of types for the 10 runs is depicted, as well as the 95% confidence levels.

In Figs. 10 and 11 the results of two example runs of the optimization process with parsimony pressure (*GA-MRPP*) are presented. Here the same format as Fig. 6 was used. Namely, the average fitness of the population (Figs. 10(a)

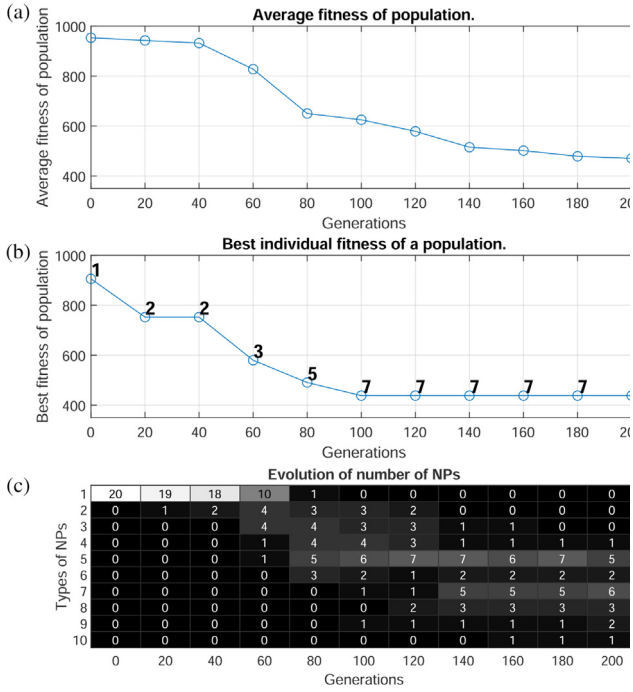

Fig. 10 – Results from one run of *GA-MRPP*; (a) Evolution of average fitness of the population; (b) evolution of the best individual in the population (where numbers indicate the number of types NPs); (c) composition of population in terms of types of NPs.

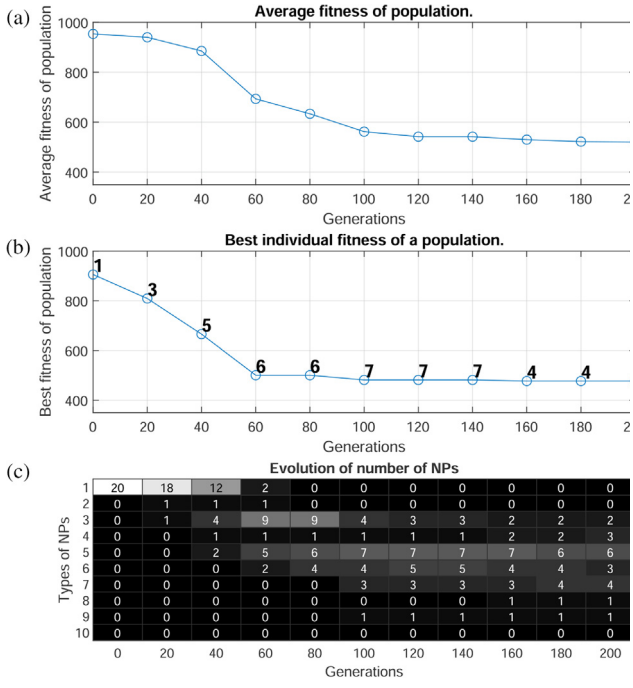

Fig. 11 – Results from one run of *GA-MRPP* where minimization of amount of NP types is observed; (a) Evolution of average fitness of the population; (b) evolution of the best individual in the population (where numbers indicate the number of types NPs); (c) composition of population in terms of types of NPs.

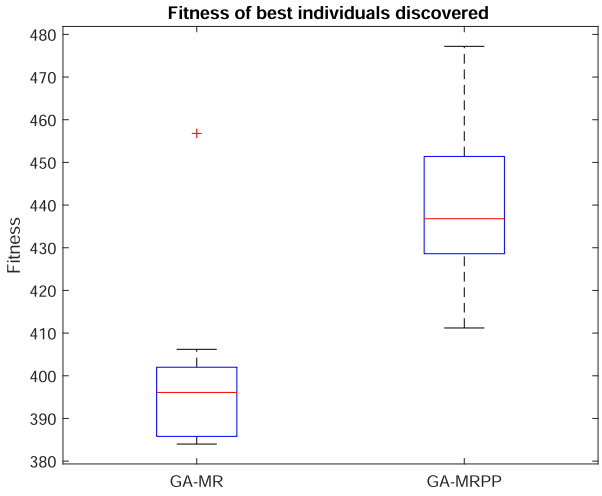

Fig. 12 – Fitness of best individual found by both variations of the metameric representation algorithms.

and 11)) and the fitness of the best individual (Figs. 10(b) and 11(b)) are depicted. Also, the composition of each best solution per generation is depicted as a number by the data point in the graph (Figs. 10(b) and 11)) and the composition of the population in terms of types of NPs is provided (Figs. 10(c) and 11(c)).

The comparison of the fitness achieved by solutions found by the two variations is illustrated in Fig. 12. Namely, summary statistics are visualized with a boxplot, for the final best individuals fitness found from both methods. The median, the 25th and 75th percentiles, minimum and maximum and one outlier for *GA-MR* (i.e. a value that is more than 1.5 times the interquartile range) are illustrated.

5. Discussion

Utilizing the *GA-MR* method the optimization of the multi NP based cancer treatments can be realized, as the average fitness (Fig. 4(a)) of the population of solutions converges to 420 remaining cancer cell agents, while the average fitness of the initial random population was 950, i.e. a 56% reduction. An additional metric of the improvement of the *in silico* optimized designs, can be realized by the fitness of the best individuals found throughout the simulated evolution (Fig. 4(b)). Namely, the fitness of the best solution in the initial population was 905 remaining cancer cell agents, while in the final population was 400, an improvement of 56%.

However, investigating closer the composition of the best solutions in the population, in terms of the amount of different NP types (Fig. 5) an unwanted effect of metameric representations methods is observed. As described previously, all tests start with a population of solutions with minimal complexity (only one type of NPs), while the amount is steadily increasing and as it can be observed it is finally reaching the maximum of 10 types. This is an indication of bloat in the results provided by this methodology (*GA-MR*).

The results of one of the test runs of *GA-MR* were closely inspected in Fig. 6. The average fitness of the population seems to converge to 420 remaining cancer cell agents

(Fig. 6(a)), while the fitness of the best individual reaches 390 at the end of the evolution (Fig. 6(a)). Inspecting the composition of each best solution per generation (Fig. 6(b)) it is obvious that from the 80th population onward, no significant improvement of the fitness is achieved, while the amount of types of NPs keep increasing. Nonetheless, from Fig. 6(c), it can be derived that the population does not converge to one amount of NPs, as there are several individuals in the area between 7 and 10 types of NPs at the final generation.

To further inspect the results at the end of the evolution, after 200 generations, Fig. 7 is presented. Here the fact that bloat is introduced by the methodology is clear. Despite the best fitness individual is of 10 types of NPs (with 390.6 remaining cancer cell agents), other solutions with 8 and 9 types of NPs are not that far behind (with 393 and 392.8 agents, respectively).

To alleviate the bloat phenomena and, thus, discover an effective treatment with lower complexity, parsimony pressure was included in the replacement operator (*GA-MRPP*). As described previously, a weight of 10% more effective behaviour needs to be presented by a new individuals with longer genome lengths, in order to replace old individuals existing in the population. Moreover, the mutation operator was updated to remove, as well as add one random type of NPs, that serves as an additional measure against bloat.

For this method of optimization, the average fitness of the population (Fig. 8(a)) reaches 470 remaining cancer cell agents, with an initial value of 950, a 50.5% reduction. Moreover, for the fitness of the best individuals (Fig. 8(b)), the initial fitness of the best solution was 905 remaining cancer cell agents, while in the final one 438, a 51.5% reduction.

On the other hand, examining the composition of the best solutions in a population (illustrated in Fig. 9), the control of bloat effect is obvious. Comparing these with the results before parsimony pressure was added (Fig. 5), it can be established that the amount of types of NPs per best solution is increasing in a more manageable way and the range is broader than previously. Thus, more diverse solutions are considered and the search does not get stuck in a local optimum, early in the evolution procedure.

Furthermore, exploring further the results of individual runs of the optimization process with parsimony pressure (Figs. 10 and 11) the mechanics of *GA-MRPP* can be realized. In Fig. 10 (same format as Fig. 6) a more gradual minimization of the fitness function can be observed, along with the controlled increase in the complexity of the treatment. Namely, the number of NP types for the best individuals found is converging to 7 (as illustrated Fig. 10(b)), while a diverse population is still existing during the last generation of the evolution (individuals with genome length from 4 to 10 types of NPs, as depicted in Fig. 10(c)). An advantage of the continuation of more diverse populations can also be realised in the *GA-MRPP* run described in Fig. 11. In Fig. 11(b) the fitness of the best treatment found per generation can be monitored, where a gradual improvement is apparent. However, after reaching a best solution of 7 types of NPs by generation 100, the methodology discovers an equally fit (and slightly better) treatment that is not as complex, namely it has only 4 types of NPs. This can be also realized in Fig. 11(c), where there seem to be only one individual with 4 types of NPs by generation 100, but due to parsimony pressure, it was not abandoned/extinct (because its fitness would be comparable with the more complex treatments), and it was given time (simulated generations) to mutate and improve its fitness, so as to become the best in the population by the end of the evolution.

The comparison of the fitness achieved by solutions found by the two variations (Fig. 12) reveals that the *GA-MRPP* variation provides not as fit solutions. Nonetheless, given that the difference is relatively small (note that *GA-MR* achieves 56% improvement as mentioned previously and median value of 396 agents, while *GA-MRPP* achieves 51.5% improvement and median value of 437), the benefits of developing less complex treatments may overshadow the small performance difference.

The trade-off between overly complex and efficient treatments can be inspected by the *GA-MRPP* methodology via altering the weight of the parsimony pressure, here set to 10%. This analysis is an aspect of future work. Moreover, a fabrication cost investigation and an *in vitro* analysis and association between the toxicity and the complexity of NP-based treatments will inform the optimization methodology to adjust the parsimony pressure threshold. Moreover, the application of non-parametric parsimony pressure [46] can be studied. The implementation of more specialized operators [47] designed for metameric representations, can be a further possible way towards future work.

The ultimate goal of any work on modelling of cancer treatments is to become integrated into pre-clinical and clinical practice as a decision support tool. This can be achieved only when models are tightly integrated with reproducible, quantitative, and dynamic biological measurements [48]. However, for that, we need a paradigm shift in how we collect, standardize and report patient data [49] and the entire field of mathematical oncology is just taking its first steps towards that goal [50]. With the application of nanomedicine, the complexity of the problem is even higher. Biodistribution and efficacy of applied drugs are significantly influenced by the nanocarrier parameters such as size, physicochemical properties and *in vivo* stability (for a comprehensive review of utilization of different biomimetic, organic, and inorganic nanocarriers see [51]). Fine-tuning of nanocarrier properties is especially important since nanomedicines should overcome numerous transport barriers in the body, starting from the circulation in the bloodstream all the way down to the release of their active cargo [28]. Because of these additional factors, the state space of possible treatment configurations is enormous. To more efficiently explore it, we need a novel set of tools. Depending on the size of the parameter space, these tools can be based either on high-throughput testing [52] or machine learning [39,53,54].

As previously stated, in contrast to existing body of work, here we focused on developing the method for automated optimization of nanocarrier properties. To the best of the authors' knowledge, at the time of writing, there are no computational models nor pre-clinical or clinical studies that compare the efficacy of utilization of multiple differentiated nanocarriers as mediators of the same chemical compound as a chemotherapeutic agent, as done in this paper. Nonetheless, because of the increasing popularity of the higher com-

plexity of cancer therapies (i.e. binding multiple drugs and functionalities in a single NP) and in specific in the area of cancer immunotherapy [51,18], diagnostics [2] and combinatorial therapies (i.e. NPs delivering chemotherapeutics and at the same time acting as a radiosensitizer [19] or photothermal and immune co-therapy [17]), the consideration of an implementation of differentiated NP-based anti-cancer chemotherapy is highly anticipated.

6. Conclusion

This study introduces an *in silico* evolutionary optimization of a multi-NP-based drug delivery system in targeted cancer treatment with a modified version of simulator PhysiCell. As PhysiCell is an open-source tool, appropriate alternations in the source code were made to simultaneously introduce multiple types of NPs in the simulated treatment. Given that the amount of different types of NPs that will provide the best treatment is not known *a priori*, a variable length evolutionary methodology is utilized, namely metameric representation.

The appropriately designed crossover and mutation operators to access the variable length genome of the individuals, required by the metameric representation, were implemented. A crossover operator with a simple alternation was utilized, known as "cut and splice" crossover, while the functionality of adding or removing a type of NP was supplemented to the mutation operator. The initial results uncontrollably increased the complexity of the solutions (comprising of the maximum amount of NPs, namely 10) and achieved increased effectiveness. However, bloat was detected in the results, meaning that the maximum of solution length was reached, without a significant improvement in the fitness.

In order to control bloat, parsimony pressure (*GA-MRPP*) was applied as an alternation to the optimization process. The results provided after enforcing these measures provided slightly less fit, but comparable treatments. Namely, an average of 56% improvement of the fitness of best individuals found with *GA-MR* was realised, while an average of 51.5% was realised with *GA-MRPP*. Despite that, while *GA-MR* discovers overly complex treatments that include the maximum of 10 types of NPs simultaneously applied, the *GA-MRPP* discovers less complex treatments with an average of 8 types of NPs. Nonetheless, the *GA-MRPP* methodology manages to converge to treatments comprised by a minimum of 4 types of NPs that are possible to secure clinical approval easier, due to limited consequences of mutual interaction.

CRediT authorship contribution statement

Michail-Antisthenis Tsompanas: Conceptualization, Investigation, Methodology, Writing - review & editing, Software, Visualization, Writing - original draft. **Larry Bull:** Conceptualization, Investigation, Methodology, Writing - review & editing. **Andrew Adamatzky:** Conceptualization, Investigation, Methodology, Writing - review & editing, Funding acquisition, Project administration, Supervision. **Igor Balaz:** Conceptualization, Investigation, Methodology, Writing - review & editing, Funding acquisition, Project administration, Supervision.

Declaration of Competing Interest

The authors declare that they have no known competing financial interests or personal relationships that could have appeared to influence the work reported in this paper.

Acknowledgements

This work was supported by the European Research Council under the European Union's Horizon 2020 research and innovation programme under grant agreement No. 800983.

REFERENCES

[1] Swain S, Kumar Sahu P, Beg S, Manohar Babu S. Nanoparticles for cancer targeting: current and future directions. Curr Drug Deliv 2016;13(8):1290–302.
[2] Zhang Y, Li M, Gao X, Chen Y, Liu T. Nanotechnology in cancer diagnosis: progress, challenges and opportunities. J Hematol Oncol 2019;12(1):137.
[3] Sztandera K, Gorzkiewicz M, Klajnert-Maculewicz B. Gold nanoparticles in cancer treatment. Mol Pharmaceutics 2018;16(1):1–23.
[4] Rodrigues CF, Jacinto TA, Moreira AF, Costa EC, Miguel SP, Correia IJ. Functionalization of AuMSS nanorods towards more effective cancer therapies. Nano Res 2019;12(4):719–32.
[5] Pairoj S, Damrongsak P, Damrongsak B, Jinawath N, Kaewkhaw R, Leelawattananon T, Ruttanasirawit C, Locharoenrat K. Antiradical properties of chemo drug, carboplatin, in cooperation with zno nanoparticles under uv irradiation in putative model of cancer cells. Biocybernetics Biomed Eng 2019;39(3):893–901.
[6] Borkowska M, Siek M, Kolygina DV, Sobolev YI, Lach S, Kumar S, Cho Y-K, Kandere-Grzybowska K, Grzybowski BA. Targeted crystallization of mixed-charge nanoparticles in lysosomes induces selective death of cancer cells. Nat Nanotechnol 2020;15(4):331–41.
[7] Zhao X, Yang K, Zhao R, Ji T, Wang X, Yang X, et al. Inducing enhanced immunogenic cell death with nanocarrier-based drug delivery systems for pancreatic cancer therapy. Biomaterials 2016;102:187–97.
[8] Minion LE, Chase DM, Farley JH, Willmott LJ, Monk BJ. Safety and efficacy of salvage nano-particle albumin bound paclitaxel in recurrent cervical cancer: a feasibility study. Gynecol Oncol Res Practice 2016;3(1):1–4.
[9] Puja P, Vinita NM, Devan U, Velangani AJ, Srinivasan P, Yuvakkumar R, Arul Prakash P, Kumar P, Fluorescence microscopy-based analysis of apoptosis induced by platinum nanoparticles against breast cancer cells, Appl Organometallic Chem 34 (9) (2020) e5740. .
[10] Tabassum DP, Polyak K. Tumorigenesis: it takes a village. Nat Rev Cancer 2015;15(8):473–83.
[11] Groten J, Venkatraman A, Mertelsmann R. Chapter 12 – modeling and simulating carcinogenesis. In: Deigner H-P, Kohl M, editors. Precision Medicine. Academic Press; 2018. p. 277–95. https://doi.org/10.1016/B978-0-12-805364-5.00012-3.
[12] Makale MT, Kesari S, Wrasidlo W. The autonomic nervous system and cancer, Biocybernetics and Biomedical. Engineering 2017;37(3):443–52.
[13] Gener P, Montero S, Xandri-Monje H, Díaz-Riascos ZV, Rafael D, Andrade F, et al. ZileutonTM loaded in polymer micelles effectively reduce breast cancer circulating tumor cells and

intratumoral cancer stem cells, Nanomedicine: Nanotechnology. Biology Med 2020;24 102106.
[14] Persidis A. Cancer multidrug resistance. Nature Biotechnol 1999;17(1):94–5.
[15] Eyler CE, Rich JN. Survival of the fittest: cancer stem cells in therapeutic resistance and angiogenesis, Journal of clinical oncology: official journal of the American Society of. Clinical Oncol 2008;26(17):2839.
[16] Easwaran H, Tsai H-C, Baylin SB. Cancer epigenetics: tumor heterogeneity, plasticity of stem-like states, and drug resistance. Mol Cell 2014;54(5):716–27.
[17] Li Y, Liu X, Pan W, Li N, Tang B. Photothermal therapy-induced immunogenic cell death based on natural melanin nanoparticles against breast cancer. Chem Commun 2020;56 (9):1389–92.
[18] Yoon HY, Selvan ST, Yang Y, Kim MJ, Yi DK, Kwon IC, Kim K. Engineering nanoparticle strategies for effective cancer immunotherapy. Biomaterials 2018;178:597–607.
[19] Yang C, Bromma K, Di Ciano-Oliveira C, Zafarana G, van Prooijen M, Chithrani DB. Gold nanoparticle mediated combined cancer therapy. Cancer Nanotechnol 2018;9 (1):1–14.
[20] Ma L, Kohli M, Smith A. Nanoparticles for combination drug therapy. ACS Nano 2013;7(11):9518–25.
[21] Zhang RX, Wong HL, Xue HY, Eoh JY, Wu XY. Nanomedicine of synergistic drug combinations for cancer therapy–strategies and perspectives. J Controlled Release 2016;240:489–503.
[22] Shrestha B, Tang L, Romero G. Nanoparticles-mediated combination therapies for cancer treatment. Adv Ther 2019;2 (11):1900076.
[23] Parhi P, Mohanty C, Sahoo SK. Nanotechnology-based combinational drug delivery: an emerging approach for cancer therapy. Drug Discovery Today 2012;17(17–18):1044–52.
[24] Jaeger S, Igea A, Arroyo R, Alcalde V, Canovas B, Orozco M, Nebreda AR, Aloy P. Quantification of pathway cross-talk reveals novel synergistic drug combinations for breast cancer. Cancer Res 2017;77(2):459–69.
[25] Nevala WK, Butterfield JT, Sutor SL, Knauer DJ, Markovic SN. Antibody-targeted paclitaxel loaded nanoparticles for the treatment of cd20+ b-cell lymphoma. Sci Rep 2017;7:45682.
[26] Sykes EA, Dai Q, Sarsons CD, Chen J, Rocheleau JV, Hwang DM, Zheng G, Cramb DT, Rinker KD, Chan WC. Tailoring nanoparticle designs to target cancer based on tumor pathophysiology. Proc Nat Acad Sci 2016;113(9):E1142–51.
[27] Dogra P, Butner JD, Chuang Y-L, Caserta S, Goel S, Brinker CJ, Cristini V, Wang Z. Mathematical modeling in cancer nanomedicine: a review. Biomed. Microdevices 2019;21(2):40.
[28] Stillman NR, Kovacevic M, Balaz I, Hauert S, In silico modelling of cancer nanomedicine, across scales and transport barriers, NPJ Comput Mater 6 (92) (2020). doi:10.1038/s41524-020-00366-8. .
[29] Johnston ST, Faria M, Crampin EJ. Isolating the sources of heterogeneity in nano-engineered particle–cell interactions. J R Soc Interface 2020;17(166):20200221.
[30] Ghaffarizadeh A, Heiland R, Friedman SH, Mumenthaler SM, Macklin P. Physicell: An open source physics-based cell simulator for 3-d multicellular systems. PLoS Comput Biol. 2018;14(2) e1005991.
[31] Ryerkerk ML, Averill RC, Deb K, Goodman ED. Solving metameric variable-length optimization problems using genetic algorithms. Genet Program Evolvable Mach 2017;18 (2):247–77.
[32] Ryerkerk ML, Averill RC, Deb K, Goodman ED. A survey of evolutionary algorithms using metameric representations. Genet Program Evolvable Mach 2019;20(4):441–78.
[33] Preen RJ, Bull L, Adamatzky A. Towards an evolvable cancer treatment simulator. BioSystems 2019;182:1–7.
[34] Tsompanas M-A, Bull L, Adamatzky A, Balaz I, Haploid-diploid evolution: Nature's memetic algorithm, arXiv preprint arXiv:1911.07302 (2019).
[35] Tsompanas M-A, Bull L, Adamatzky A, Balaz I, Utilizing differential evolution into optimizing targeted cancer treatments, arXiv preprint arXiv:2003.11623 (2020).
[36] Tsompanas M-A, Bull L, Adamatzky A, Balaz I. Novelty search employed into the development of cancer treatment simulations. Inform Med Unlocked 2020 100347.
[37] Ozik J, Collier N, Heiland R, An G, Macklin P. Learning-accelerated discovery of immune-tumour interactions. Mol Syst Design Eng 2019;4(4):747–60.
[38] Tsompanas M-A, Bull L, Adamatzky A, Balaz I, Evolving nano particle cancer treatments with multiple particle types, (under review) (2020).
[39] Tsompanas M-A, Bull L, Adamatzky A, Balaz I. In silico optimization of cancer therapies with multiple types of nanoparticles applied at different times. Comput Methods Programs Biomed 2020;105886.
[40] Poli R, Langdon WB, McPhee NF, Koza JR. A field guide to genetic programming. Lulu Com 2008.
[41] Wagner M, Neumann F. Parsimony pressure versus multi-objective optimization for variable length representations. In: International Conference on Parallel Problem Solving from Nature. Springer; 2012. p. 133–42.
[42] Mora JC, Barón JMC, Santos JMR, Payán MB. An evolutive algorithm for wind farm optimal design. Neurocomputing 2007;70(16–18):2651–8.
[43] Weicker N, Szabo G, Weicker K, Widmayer P. Evolutionary multiobjective optimization for base station transmitter placement with frequency assignment. IEEE Trans Evol Comput 2003;7(2):189–203.
[44] Stanley KO, Miikkulainen R. Evolving neural networks through augmenting topologies. Evol Comput 2002;10 (2):99–127.
[45] PhysiCell: An open source physics-based cell simulator, http://physicell.org/, [Online; accessed Jan-2020] (2020). .
[46] Luke S, Panait L. Fighting bloat with nonparametric parsimony pressure. In: International Conference on Parallel Problem Solving from Nature. Springer; 2002. p. 411–21.
[47] Ryerkerk M, Averill R, Deb K, Goodman E. A novel selection mechanism for evolutionary algorithms with metameric variable-length representations. Soft Comput 2020:1–14.
[48] Fong EJ, Strelez C, Mumenthaler SM. A perspective on expanding our understanding of cancer treatments by integrating approaches from the biological and physical sciences. SLAS DISCOVERY: Adv Sci Drug Discovery 2020;25 (7):672–83.
[49] Anderson AR, Maini PK. Mathematical oncology. Bull Math Biol 2018;80(5):945–53.
[50] Enderling H, Alfonso JCL, Moros E, Caudell JJ, Harrison LB. Integrating mathematical modeling into the roadmap for personalized adaptive radiation therapy. Trends Cancer 2019;5(8):467–74.
[51] Hao Y, Zhou X, Li R, Song Z, Min Y. Advances of functional nanomaterials for cancer immunotherapeutic applications. Wiley Interdisciplinary Rev: Nanomedicine Nanobiotechnol 2020;12(2) e1574.
[52] Ozik J, Collier N, Wozniak JM, Macal C, Cockrell C, Friedman SH, Ghaffarizadeh A, Heiland R, An G, Macklin P. High-throughput cancer hypothesis testing with an integrated physicell-emews workflow. BMC Bioinform 2018;19(18):81–97.
[53] Balaz I, Petrić T, Kovacevic M, Tsompanas M-A, Stillman N. Harnessing adaptive novelty for automated generation of cancer treatments. Biosystems 2021;199 104290.
[54] Benzekry S. Artificial intelligence and mechanistic modeling for clinical decision making in oncology. Clinical Pharmacol Ther 2020;108(3):471–86.